Energy & Environmental Science

Cite this: *Energy Environ. Sci.*, 2012, **5**, 6933

www.rsc.org/ees

PAPER

Enveloping porphyrins for efficient dye-sensitized solar cells†

Chin-Li Wang,[a] Chi-Ming Lan,[b] Shang-Hao Hong,[a] Yi-Fen Wang,[a] Tsung-Yu Pan,[b] Chia-Wei Chang,[b] Hshin-Hui Kuo,[a] Ming-Yu Kuo,*[a] Eric Wei-Guang Diau*[b] and Ching-Yao Lin*[a]

Received 28th November 2011, Accepted 1st February 2012
DOI: 10.1039/c2ee03308a

A series of porphyrins bearing alkoxyl and/or alkyl chains were prepared to investigate the roles of alkoxyl/alkyl chains in the enhanced photovoltaic performance of the dyes. Based on the experimental results and the molecular simulations, we demonstrated that suitable long alkoxyl chains are capable of wrapping the porphyrin core, thus resulting in decreased dye aggregation, elevated excited states and LUMOs, and improved photovoltaic performance.

Introduction

Dye-sensitized solar cells (DSSCs) have been of great interest because they present a promising alternative to conventional photovoltaic devices based on silicon.[1–5] The solar energy to electric power conversion efficiencies (η) greater than 11% have been demonstrated with DSSCs sensitized by polypyridyl ruthenium complexes.[6–8] On the other hand, numerous novel sensitizers have also been intensely investigated for their modest cost, ease of synthesis and modification, large molar absorption coefficients and satisfactory stability. Among the dyes under investigation, porphyrins are considered as one of the more efficient sensitizers for DSSC applications[9–22] because of the vital roles of porphyrin derivatives in photosynthesis, the strong absorption in the visible region, and the ease of adjusting the chemical structures for light harvest. During the development of porphyrin photo-sensitizers, Campbell *et al.* were the first to raise the overall efficiency of porphyrin-sensitized solar cells (PSSCs) to 7.1% by using a side-anchoring and fully conjugated dye.[12] In 2010, Bessho *et al.* further raised the overall efficiency of PSSC to 11% based on a push–pull molecular design.[13]

In an attempt to create efficient porphyrin dyes, our systematic studies have shown that higher photovoltaic performance of a zinc porphyrin can be achieved by attaching an anchoring group with a shorter spacer (dye labelled as PE1),[18a] by incorporating a π-conjugated acene group to extend the light-harvesting spectral range (LAC3),[19] by applying an electron-donating group (LD13),[20] or by adding a poly aromatic group to the π-conjugation system (LD4).[21] Although the device made of the LD4 dye showed an overall efficiency greater than 10%,[21] we have noticed that the photovoltaic performance of certain planar porphyrin dyes might be further improved by decreasing the degree of dye aggregation.[18c] In order to achieve such a goal, we designed porphyrin derivatives with long alkoxyl or alkyl groups for dye insulation. Long alkoxyl or alkyl chains have a long-standing reputation of increasing the solubility of chromophores for various applications. For example, the pioneering works of Hupp and co-workers have demonstrated that phenyl groups

[a]*Department of Applied Chemistry, National Chi Nan University, Puli, Nantou Hsien 54561, Taiwan. E-mail: cyl@ncnu.edu.tw; mykuo@ncnu.edu.tw; Fax: +886-49-2917956; Tel: +886-49-2910960 ext. 4152*
[b]*Department of Applied Chemistry and Institute of Molecular Science, National Chiao Tung University, Hsinchu 30010, Taiwan. E-mail: diau@mail.nctu.edu.tw; Fax: +886-3-5723764; Tel: +886-3-5131524*

† Electronic supplementary information (ESI) available: Experimental details including the synthesis and characterization of the LD dyes, stability tests of LD16 solar cells under ambient conditions for 1000 hours, and a full size figure of Scheme 2. See DOI: 10.1039/c2ee03308a

Broader context

Dye-sensitized solar cells have been known to exceed the 10% device overall efficiency barrier with Ru-based photo-sensitizers. Recently, several studies have reported porphyrins as efficient photo-sensitizers with comparable photovoltaic performance to that of the Ru complexes. However, like all other planar dyes, porphyrins aggregate easily in the solutions at higher concentration. As we attempted to increase the dye-loading of porphyrin-sensitized solar cells to boost the overall efficiencies of the devices, we encountered severe molecular aggregation problems which might likely hamper power conversion efficiencies of the solar cells. In order to remedy this issue, we demonstrate in this work that molecular aggregation of a planar photo-sensitizer in the solutions can be significantly reduced by wrapping the dye with suitable long alkyl chains. As a result, the properly insulated porphyrin dyes show lessened aggregation, elevated singlet excited states and LUMOs, and much improved photovoltaic performance. Our studies also show that attaching long alkyl chains at the top of the porphyrins slightly improves their performance.

bearing *ortho*-alkoxyl chains can effectively decrease porphyrin aggregation for supramolecular applications.[23] Likewise, Therien and co-workers used 2′,6′-bis(3,3-dimethyl-1-butyloxy)phenyl groups to increase the solubility of several porphyrin arrays.[24] By different approaches, Osuka and co-workers reported a doubly strapped porphyrin to study dye encapsulation and "steric protection" for phosphorescent dopants in OLEDs.[25] Imahori and co-workers investigated the size effects of porphyrin substituents and adsorption conditions on the photovoltaic properties of PSSC.[10e] Galoppini's group has been systematically investigating the effects of chromophore insulation on the surfaces of semiconductors by "capped", "strapped" or "guest–host" molecular design.[11,26] Recently, small organic dyes with long alkyl substituents have been reported to feature good solubility in organic solvents and high DSSC performance.[27–30] Finally, thermally stable amphiphilic ruthenium dyes such as Z907 and C101–C107 dye also benefit from using long alkyl groups in the molecular design.[8,27]

By introducing long alkoxyl chains into our systems, we have shown that the photovoltaic performance of a zinc porphyrin can be significantly enhanced by *ortho*-alkoxylated phenyl groups at the macrocyclic *meso*-positions. An overall efficiency greater than 10% was attained (LD14).[22] In contrast, we observed inferior photovoltaic properties of porphyrins with *meta*/*para*-substituted phenyl rings. The superior performance of the LD14 dye over that of the *meta*-substituted counterpart (LD13) was attributed to the alkoxyl chains wrapping the porphyrin core to effectively reduce dye aggregation. Most recently, Yella *et al.* reported overall efficiencies of PSSCs with cobalt(II/III)-based redox electrolyte exceeding 12%, which also took advantage of modifying a push–pull porphyrin dye with *ortho*-alkoxylated phenyl groups (YD2-oC8).[31] In the present work, we aim to uncover more details on how the alkoxyl chains affect the fundamental properties and the photovoltaic performance of the porphyrin dyes. As shown in Scheme 1, the porphyrin sensitizers under investigation are labelled as LD13–LD16. Note that we also prepared LD14 dyes with shorter alkoxyl chains, labelled as LD14-C8 and LD14-C4, in order to address the effects of the alkoxyl lengths.

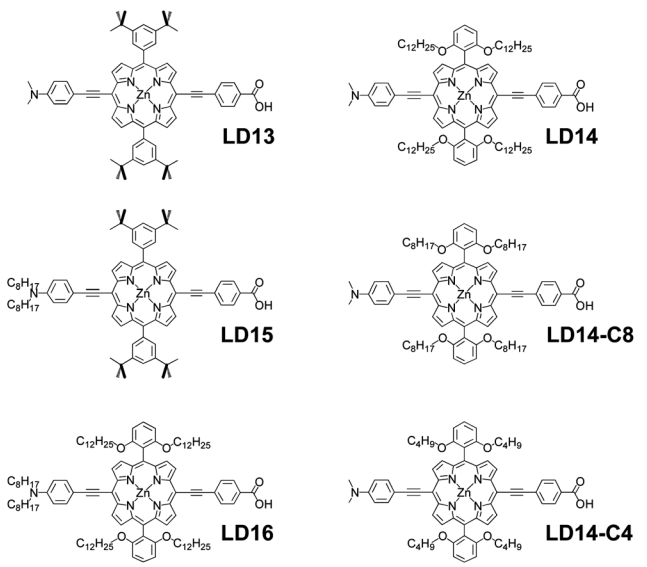

Scheme 1 Molecular structures of LD porphyrins.

Results and discussion

Molecular design and synthesis

The LD porphyrins were readily prepared in two steps according to the Sonogashira cross-coupling method (ESI†).[32] These porphyrins were designed to observe the effects of alkoxyl chains at the phenyl groups and/or the alkyl chains at the amino substituent. For example, comparison between the LD13 and LD14 dyes or the LD15 and LD16 dyes would show the effects of the four alkoxyl chains. Comparison between the LD13 and LD15 dyes or the LD14 and LD16 dyes would demonstrate the influence of the alkyl chains at the electron-donating amino group. By comparing the LD14, LD14-C8, and LD14-C4 dyes, the length effects of the alkoxyl chains can be addressed. Finally, with four long alkoxyl chains at the macrocyclic *meso*-phenyl groups and two alkyl chains added to the amino substituent, the LD16 dye represents the ultimate version of our design, a push–pull porphyrin dye with long alkoxyl/alkyl chains to increase its solubility in organic solvents.

UV-visible absorption and fluorescence spectra

As shown in Fig. 1, the LD dyes exhibit typical porphyrin absorption characteristics:[33] strong B (or Soret) bands were found near 460 nm, whereas weak Q bands were observed near 670 nm. For LD13, LD14, LD15, and LD16, both B and Q bands are only slightly shifted. As for the length effect of the alkoxyl chains, the spectra of LD14, LD14-C8, and LD14-C4 are nearly identical in THF. This indicates that the alkoxyl/alkyl chains have little effect on the porphyrin UV-visible spectra.

Fig. 2a shows the B band-excited fluorescent emission spectra of LD13, LD14, LD15, and LD16, and Fig. 2b overlays those of LD14, LD14-C8, and LD14-C4. The emission maxima are given in Table 1. The fluorescent emissions of the LD porphyrins are found at ~680 nm. Although the intensities are comparable, the fluorescence intensities of LD14 and LD16 are slightly stronger than those of LD13 and LD15, respectively. This is consistent with the higher solubility and lessened aggregation of LD14 and LD16 in THF, indicating the effects of the four alkoxyl chains (see below). Interestingly, the fluorescence emissions of LD15

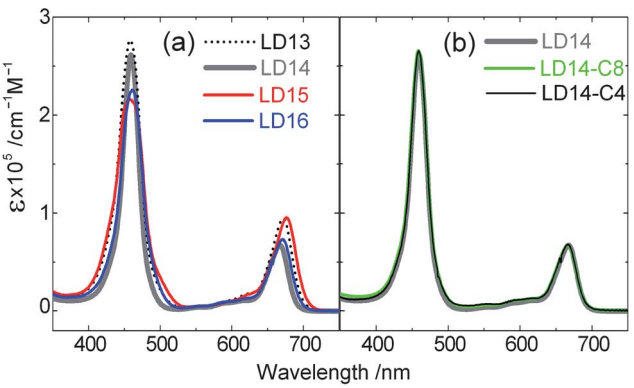

Fig. 1 Absorption spectra of LD porphyrins in THF.

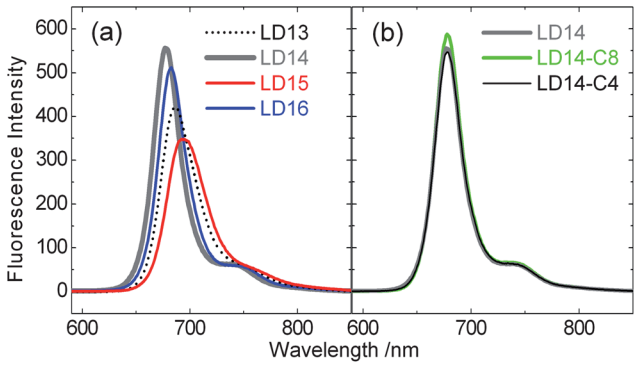

Fig. 2 B band-excited fluorescent emission spectra of LD porphyrins (2.0×10^{-6} M in THF).

and LD16 are less intense than those of LD13 and LD14, respectively. This might be related to the long alkyl chains of the amino groups. In contrast, the fluorescent spectra of LD14, LD14-C8, and LD14-C4 in THF are nearly identical. This indicates that the lengths of the alkoxyl/alkyl chains have no dramatic effects on the fluorescent emissions of the LD porphyrins in THF.

Fig. 3 compares the UV-visible spectra of LD porphyrins in THF with those on TiO_2 films in air. Table 2 shows the full widths at half maximum (FWHM) of these absorption bands in THF and on TiO_2 films. Note that only small amounts of the LD porphyrins were allowed to adsorb onto the TiO_2 films to prevent saturation of the B-band absorptions in the spectra. In addition, these absorption bands were all normalized in order to make a more visible comparison. For LD13 and LD15, the B and Q bands of the film spectra were only slightly shifted but considerably broadened relative to their solution counterparts. The broadened features of the film samples are consistent with intermolecular interactions of molecules aggregated on TiO_2.[34,18b] In contrast, the absorption bands of the LD14 film are relatively sharp compared to those in the solution spectrum (Fig. 3d). This is consistent with the literature reports of similar complexes,[23] suggesting that the four *ortho*-alkoxyl chains at the two *meso*-phenyl groups effectively reduce the aggregation of the LD14 dye. As for the length effects of the alkoxyl chains, comparison of Fig. 3d–f and Table 2 clearly shows that the blue-shoulder of the porphyrin B bands becomes more obvious as the lengths of the alkoxyl chains decrease. Because the blue shoulders represent H-type aggregation of the porphyrins on

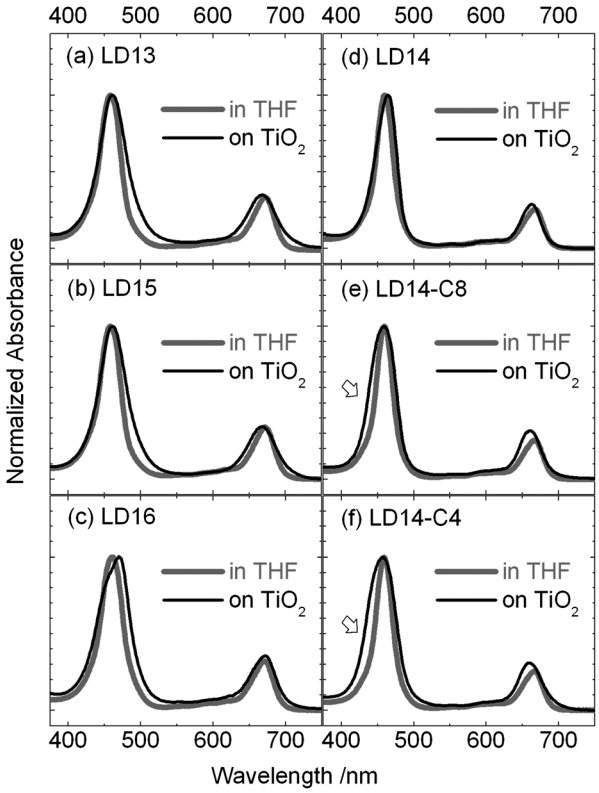

Fig. 3 Normalized UV-visible spectra of LD porphyrins in THF (grey curves) and on TiO_2 films in air (black curves). The arrows in (e) and (f) suggest the more evident H-type aggregation responses of the porphyrins.

TiO_2,[18b,34] the lack of such feature in the LD14 film spectrum suggests lessened H-type aggregation of LD14 on TiO_2. Accordingly, the re-appearance of the B band blue-shoulders in the LD14-C4 and LD14-C8 spectra suggests that the aggregation of LD porphyrins becomes more severe as the lengths of the alkoxyl chains decrease. As will be addressed later in the simulation section, this increased aggregation phenomenon may be due to less coverage provided by the shorter alkoxyl chains. This suggestion is consistent with the crystal structures reported for porphyrins with shorter alkoxyl chains.[23,24,35] In contrast to the LD14's sharp film spectrum, the LD16 film spectrum shows more broadened and split Soret bands. The blue-shifted and red-shifted spectral features suggest H-type and J-type aggregations[34] of the LD16 molecules on the surface of TiO_2, respectively. This

Table 1 Absorption wavelength, fluorescence maxima and first porphyrin-ring redox potentials of LD porphyrins in THF

			$E_{1/2}$/V *vs.* SCE[b]	
Dye	Absorption/nm (log ε, M^{-1} cm^{-1})	Emission[a]/nm	Ox(1)	Red(1)
LD13	458(5.44), 672(4.98)	685	+0.81	−1.15
LD14	459(5.40), 667(4.82)	677, 740	+0.74	−1.32
LD15	457(5.33), 677(4.78)	695	+0.79	−1.15
LD16	461(5.35), 671(5.86)	683, 746	+0.72	−1.32
LD14-C8	459(5.42), 667(4.83)	678, 739	+0.73	−1.31
LD14-C4	459(5.42), 667(4.83)	678, 739	+0.74	−1.30

[a] 2.0×10^{-6} M of LD porphyrins in THF, excitation wavelength per nm: LD13, 458; LD14, 459; LD15, 457; LD16, 461; LD14-C4, 459; LD14-C8, 459. [b] 0.5 mM of LD porphyrins in THF/0.1 M TBAP/N_2; Pt working and counter electrodes; SCE reference electrode; scan rate = 100 mV s^{-1}.

Table 2 Comparison of full width at half maximum (FWHM/cm^{-1})[a] of the LD porphyrin absorption bands in THF and on TiO_2 films

	In THF solutions		On TiO_2 films	
Dye	B/nm (FWHM)	Q/nm (FWHM)	B/nm (FWHM)	Q/nm (FWHM)
LD13	458(1670)	672(810)	461(2137)	668(1086)
LD14	459(1316)	667(708)	464(1663)	663(751)
LD15	457(1670)	677(789)	459(2992)	671(1336)
LD16	461(1721)	671(960)	470(2404)	672(1015)
LD14-C8	459(1317)	667(709)	457(2030)	658(855)
LD14-C4	459(1316)	667(708)	457(2298)	659(1086)

[a] From Fig. 3.

interesting phenomenon will be further addressed later in the simulation section.

Electrochemical properties and energy levels

Fig. 4 shows the cyclic voltammograms (CV) of the LD porphyrins in THF. The first redox potentials of these complexes are listed in Table 1. The first porphyrin-ring reductions of LD13 and LD15 are found at −1.15 V *vs.* SCE as *quasi*-reversible reactions, whereas those of LD14 and LD16 are located at −1.32 V *vs.* SCE. These values are consistent with the formation of a zinc porphyrin anion radical.[24,36,37] As for LD14, LD14-C8, and LD14-C4, the first porphyrin-ring reduction potentials are determined to be at −1.32, −1.31, and −1.30 V *vs.* SCE, respectively. The very slight anodic shift of these reduction potentials suggests minimal influence of the alkoxyl lengths to the porphyrin LUMO energy levels. For the oxidation reactions, two waves of *quasi*-reversible reactions are observed for the LD porphyrins. The first oxidation reactions of LD13 and LD15 are observed at +0.81 and +0.79 V *vs.* SCE, whereas those of LD14 and LD16 are centred at +0.74 and +0.72 V *vs.* SCE, respectively. These values are consistent with the formation of a zinc porphyrin cation radical. The second oxidative waves have been previously established to be the reactions localized at the electron-donating amino substituents of the LD porphyrins.[20] Finally, the first oxidation potentials of LD14, LD14-C8, and LD14-C4 are determined to be at +0.74, +0.73, and +0.74 V *vs.* SCE, respectively. Again, the very limited shift of the first oxidation potentials suggests minimal influence of the alkoxyl lengths to the porphyrin HOMO energy levels.

Significantly, the CV results indicate that the first porphyrin-ring reduction potentials of LD14 and LD16 are 170 mV more negative than those of LD13 and LD15, whereas the first oxidation potentials of LD14 and LD16 are about 70 mV more negative than those of LD13 and LD15. It is logical to suggest that these cathodic shifts of the redox potentials are caused by the four alkoxyl chains. The trend is consistent with the literature reports of organic dyes bearing linear alkyl chains with various lengths.[30] The negative shifts of the LD porphyrin redox potentials should translate to higher LUMO levels and singlet excited states, contributing to a better electron injection from the dye to TiO_2. In contrast, the two amino alkyl chains do not seem to have significant effects on the porphyrin redox potentials.

Fig. 5 depicts the energy-level diagram of the LD porphyrins, comparing the ground to oxidized state (S^o/S^+) and the singlet excited state (S*) energy levels of each porphyrin with the conduction band (CB) of TiO_2 as well as the redox energy of I^-/I^{3-}. The first porphyrin-ring oxidation potentials were used to estimate the S^o/S^+ levels. Normalized Q-band absorptions and the fluorescence bands were used to estimate the energy gaps between the S* and the S^o/S^+ levels. As suggested in the figure, all

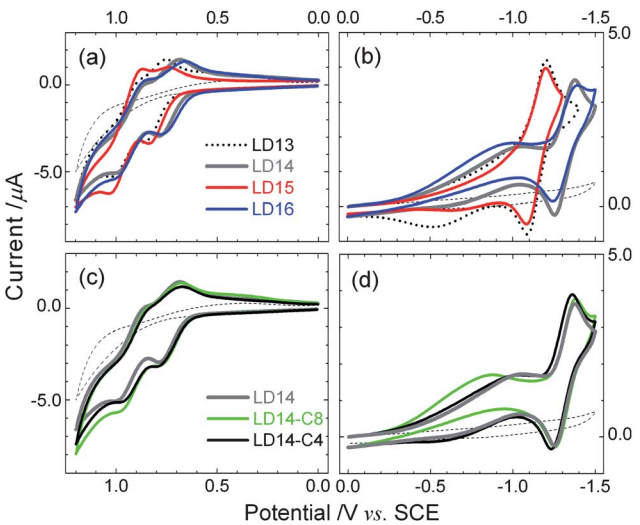

Fig. 4 Cyclic voltammograms of LD porphyrins in THF/TBAP.

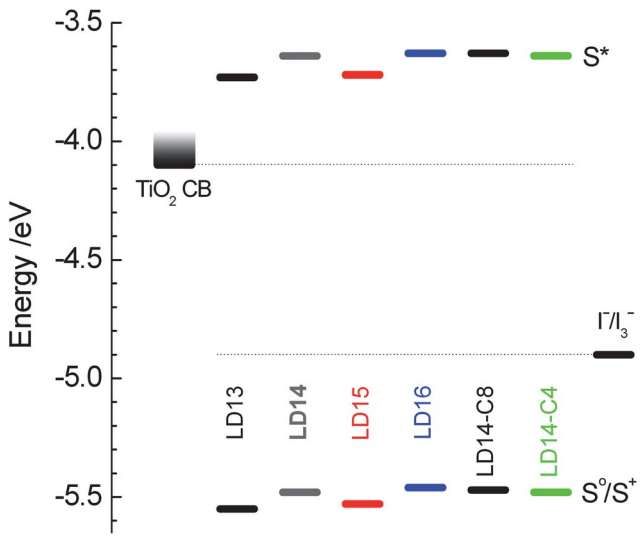

Fig. 5 Energy-level diagram of the LD dyes, the electrolyte and TiO_2.

LD porphyrins should be capable of injecting electrons to the CB of TiO_2 upon excitation. More importantly, electron injection from the dyes to TiO_2 should be more favourable for LD14 and LD16 than for LD13 and LD15 owing to the higher S* levels. This diagram also shows that the lengths of the alkoxyl chains have very small impacts on the porphyrin energy levels. Finally, energy level diagrams of the LD porphyrins *vs.* TiO_2 and I^-/I^{3-} solely based on the redox potentials are also provided in the ESI (Fig. S2†) for comparison. The patterns are very similar to those shown in Fig. 5.

Photovoltaic properties

Fig. 6a and c show the current–voltage characteristics and the corresponding IPCE action spectra for the LD14, LD15, LD16, and LD14-C8 cells, respectively, prepared with EtOH/toluene = 1/1 (v/v) as the dye-soaking solvent. On the other hand, Fig. 6b and d compare the *I–V* and the corresponding IPCE curves for the LD13, LD15, LD14-C4, and LD14-C8 devices, respectively, prepared with THF as the dye-soaking solvent. The photovoltaic parameters are listed in Table 3. The LD13 and LD14-C4 dyes are not soluble in EtOH/toluene, therefore, the devices were prepared by using THF in the dye-adsorption process. In contrast, the LD14, LD15, LD16 and LD14-C8 cells can be prepared by using either EtOH/toluene or THF as the dye-soaking solvent. For comparison, photovoltaic measurements were carried out for the LD15 and LD14-C8 cells prepared with both dye-soaking solvents.

In general, the devices prepared with EtOH/toluene as the dye-soaking solvent tend to outperform those prepared with THF. For example, we observed that the overall efficiency of the LD14-C8 devices increased from 6.39% to 8.94% when changing the dye-soaking solvent from THF to EtOH/toluene. This may be related to the greater solubility of the dye in THF than in EtOH/toluene. The strong interactions between the THF molecules and the porphyrin molecules could hamper the dye-adsorption process onto the surface of TiO_2, resulting in a poorer dye-load. We have reported that the amount of dye-loading was significantly increased when adsorbing dyes onto TiO_2 films in EtOH/toluene.[22] This phenomenon contributes to the substantially higher J_{SC} and V_{OC} values observed for the LD14-C8 cells prepared with EtOH/toluene, resulting in a higher overall efficiency. Interestingly, changing the dye-soaking solvents did not seem to greatly affect the LD15-cells and the overall efficiency was only slightly increased from 8.77% (THF) to 8.92% (EtOH/toluene).

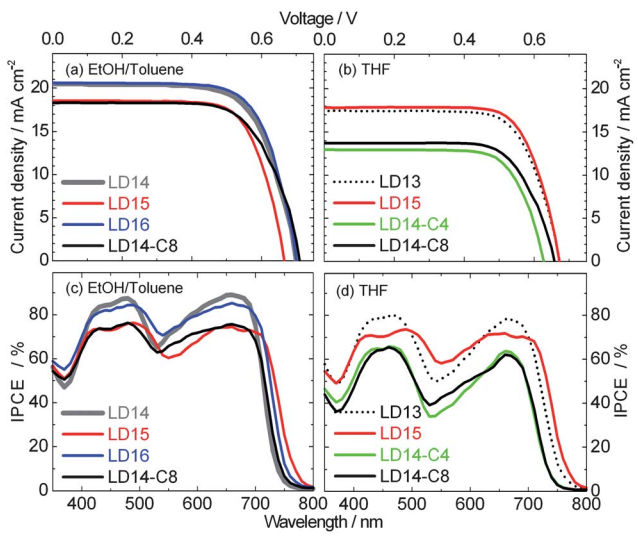

Fig. 6 Current–voltage characteristics of LD-sensitized solar cells using (a) EtOH/toluene or (b) THF as the adsorption solvents; and corresponding IPCE action spectra of LD-sensitized solar cells using (c) EtOH/toluene or (d) THF as the dye-soaking solvents.

As for the length of the alkoxyl chains, we found that the efficiencies of the solar cells exhibit a systematic trend of LD14 > LD14-C8 > LD14-C4, with the LD14 cell having an overall efficiency greater than 10%. As will be discussed in the next section, this trend should be largely related to the degree of dye insulation provided by the alkoxyl chains. On the other hand, we found that the length of the alkyl chains on the amino substitutes has only a small impact on the device performance. Nonetheless, the device efficiency slightly increased from 8.37% of LD13 to 8.92% of LD15 and from 10.05% of LD14 to 10.24% of LD16.

The remarkable photovoltaic performance of the LD14 and LD16 devices arises from their greater J_{SC} values (20.397 and 20.587 mA cm^{-2}, respectively) due to higher dye-loadings and the excellent light-harvesting ability covering the entire visible spectral region. Also, the V_{OC} of the LD14 (0.710 V) and LD16 (0.707 V) devices were noticeably higher than those of LD13 (0.676 V) and LD15 (0.669 V) cells. The enhancements in V_{OC} for both LD14 and LD16 devices should be owing to (1) more favourable electron injection from the dyes to TiO_2 (Fig. 5) and (2) retarded charge recombination accomplished by the long alkoxyl chains.[22]

Finally, we have monitored the long-term stability of the LD16 cells fabricated with a complete thermal compression assembly. The results (Fig. S1, ESI†) indicate that about 50% of the device overall efficiencies remained after 1000 hours under ambient conditions. Upon closer inspection of the parameters, we found that the V_{OC} and FF values stayed the same throughout the tests. The J_{SC} values, however, considerably dropped to about 50% of the initial values after 1000 hours. Therefore, the performance degradation of the LD16 cells over a long period of time should be related to the drop of the current output.

Simulation results

Because of the long alkoxyl/alkyl chains, obtaining crystal structures of the LD porphyrins is not feasible. More importantly, in order to visualize the alkoxyl and alkyl chains of the LD porphyrins in the solutions, molecular dynamics (MD) simulations were carried out for LD14, LD14-C8, LD16 in EtOH/toluene = 1/1 (v/v), and LD14-C4 in THF by using Materials Studio software package.[38] The MD simulation was simplified by treating the LD dyes as free-base porphyrins. Scheme 2 depicts their final structures after thermal equilibrium. As shown in the scheme, the phenyl groups at the macrocyclic *meso*-positions are fairly perpendicular to the porphyrin macrocylic planes. The dihedral angles are simulated to be between 65° and 80°. This phenomenon is due to the steric hindrance between the porphyrin core and the phenyl rings and is consistent with the reported crystal structures of various porphyrins.[23b,24c,35]

Table 3 Photovoltaic parameters of LD-sensitized solar cells[a]

Solvent	Dye	J_{SC}/mA cm^{-2}	V_{OC}/V	FF	η (%)
THF	LD13	17.432	0.676	71.03	8.37
	LD15	17.867	0.676	72.60	8.77
	LD14-C8	13.719	0.662	70.40	6.39
	LD14-C4	17.019	0.632	72.12	5.91
EtOH/toluene = 1/1 (v/v)	LD14	20.397	0.710	69.40	10.05
	LD15	18.561	0.669	71.83	8.92
	LD16	20.587	0.707	70.37	10.24
	LD14-C8	18.330	0.714	68.38	8.94

[a] Under AM1.5 illumination (power 100 mW cm^{-2}) with an active area of 0.16 cm^2.

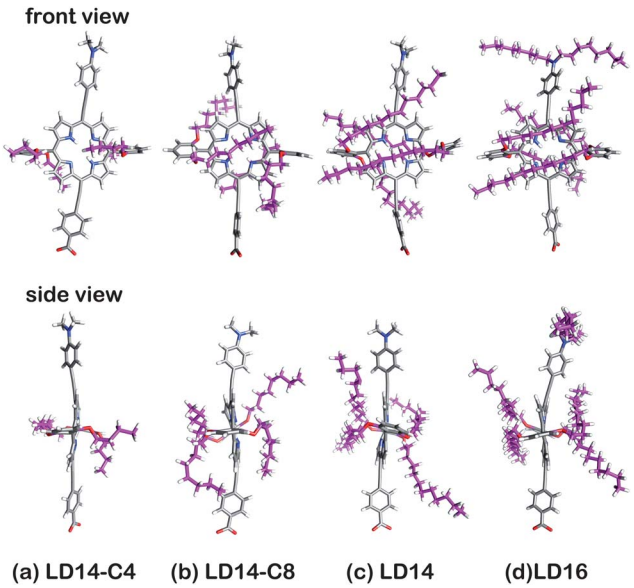

Scheme 2 Simulated molecular structures of (a) LD14-C4 in THF, and (b) LD14-C8, (c) LD14, and (d) LD16 in EtOH/toluene = 1/1 (v/v). The alkoxyl and alkyl chains are highlighted in purple.

As a result, the alkoxyl chains at the phenyl *ortho*-positions are forced to enfold around the porphyrin core. For LD14-C4, the four butoxyl chains are capable of creating cavities above and underneath the porphyrin core (Scheme 2a). This is consistent with the reported crystal structures of a number of porphyrins.[23b,c,24c,35] However, the simulation shows that the butoxyl chains are too short to completely surround the porphyrin core. In sharp contrast, the simulation shows that the porphyrin core of LD14 is fully encircled by the dodecoxyl chains. As such, the four dodecoxyl chains of LD14 should provide more effective insulation of the dye, resulting in lessened molecular aggregation and better solubility in non-coordinating organic solvents. For LD14-C8, the porphyrin core seems to be almost covered by the octoxyl chains. However, the "wrapping" in LD14-C8 is not as extensive as in LD14. In short, the MD simulations suggest that the tendency of molecular aggregation should be in the order LD14-C4 > LD14-C8 > LD14.

This trend is consistent with several experimental results: first of all, the UV-visible FWHM data show that the absorption band broadness is also in the same order: LD14-C4 > LD14-C8 > LD14 (Table 2). Since the absorption band broadening phenomenon is related to dye aggregation on the surface of TiO_2, LD14-C4's broader absorption bands support our suggestion that the dye is more aggregated than LD14. Secondly, LD14-C4 can only be handled by coordinating solvents such as THF, whereas LD14-C8 and LD14 can be used in non-coordinating EtOH/toluene co-solvents to prepare DSSCs. Thirdly, comparing the ^{1}H-NMR spectra of LD14-C4, LD14-C8, and LD14 in $CDCl_3$ (Fig. 7) reveals signal broadening phenomenon from LD14 to LD14-C4 in the aromatic region. This phenomenon is consistent with porphyrin aggregation.[39]

The simulation results are also consistent with the device performance that the overall power conversion efficiency of the LD14 cell (10.05%) is higher than those of LD14-C8 (8.94%) and LD14-C4 (5.91%) devices. It should be noted that the lower power conversion efficiency of the LD14-C4 device should result from the combined effects of significant molecular aggregation and the low solubility in non-coordinating EtOH/toluene. As a result, THF was used for the dye-soaking process and less amount of the dye was loaded onto TiO_2.[22] For LD16, the porphyrin core structure is fully wrapped by the four dodecoxyl chains. In addition, the simulations show that the extending octyl

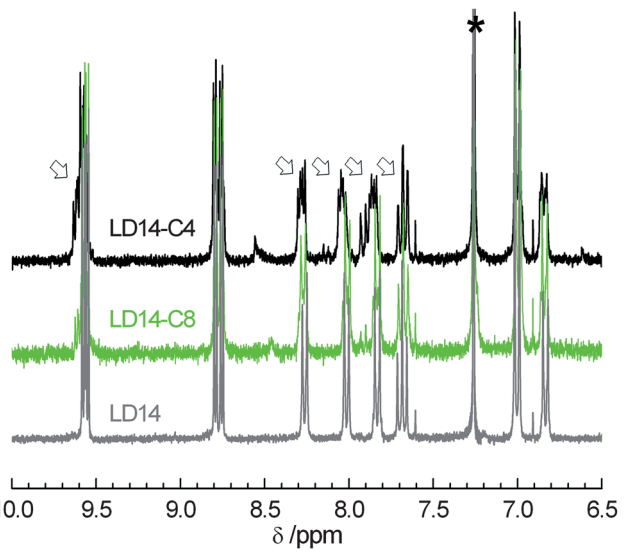

Fig. 7 ^{1}H-NMR spectra of LD14-C4 (top), LD14-C8 (middle), and LD14 (bottom) in $CDCl_3$ with trace amount of d_5-pyridine. [porphyrin] = 2.7 × 10^{-3} M. The broadened signals marked with arrows are consistent with porphyrin aggregation.

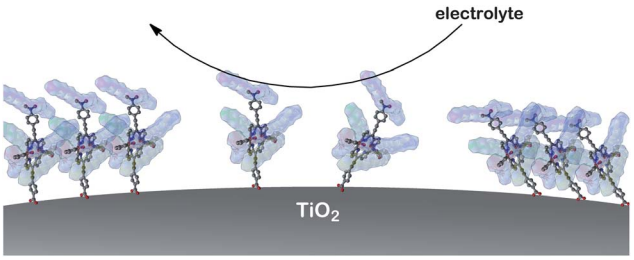

Scheme 3 Schematic illustration of a possible model of LD16 assembly on TiO_2. The colour surfaces represent the long alkoxyl/alkyl chains of LD16. Note that the surface of TiO_2 is not completely covered by LD16 to represent the experimental conditions in Fig. 3c. This scheme implies that the alkoxyl/alkyl chains could form a hydrophobic layer between the electrolyte and TiO_2 when the dyes fully cover the TiO_2 surface.

chains at the amino group should be long enough to provide additional protection of the dye from the liquid electrolyte. This additional protection is consistent with LD16's slightly superior photovoltaic performance over LD14.

To visualize LD16 on TiO_2, Scheme 3 illustrates a possible model for the assembly of LD16 dyes on the surface of TiO_2. In this scheme, simulated LD16 molecules are placed on the spherical surface of a TiO_2 nano-particle. Note that the surface of TiO_2 is not completely covered by the LD16 dyes in order to represent the experimental conditions in Fig. 3 (*i.e.* partially loaded film spectra). Therefore, some of the porphyrins are depicted as monomers and some as aggregates in the scheme. To be consistent with the split Soret bands in Fig. 3c, aggregated LD16 molecules in this scheme are arranged to feature both perpendicular (left) and tilted (right) orientations. As such, the perpendicular or tilted LD16 aggregates each represents H- or J-type molecular aggregations of LD16 dyes on the TiO_2 surface, respectively. This model is consistent with the literature reports showing the spectral evidence of porphyrin aggregated on TiO_2 in the H-[18] or J-type[10d,12b] fashion. Either way, π–π interactions between the macrocycles may not play a major role because each porphyrin is well enveloped within the alkoxyl/alkyl chains. It is worth mentioning that LD16's spectrum featuring both H- and J-types of molecular aggregation on TiO_2 may be related to the alkyl chains of the amino group. This suggestion is based on comparing the relatively sharp and slightly shifted Soret bands of the LD14 film (Fig. 3d) with the rather broadened and split Soret bands of the LD16 film (Fig. 3c). Finally, Scheme 3 also implies that a layer of alkoxyl/alkyl chains can be formed when the surface of TiO_2 is fully covered by the LD dyes. This hydrophobic layer could serve as a blocking layer between the liquid electrolyte and the TiO_2. It has been shown that creating a blocking layer between the liquid electrolyte and the electrode may create a potential barrier to retard the charge recombination process,[40] thus enhancing the photovoltages and improving the overall DSSC efficiencies. This effect has been observed in our previous report of LD14.[22]

Conclusions

We successfully prepared a series of push–pull zinc porphyrins with *ortho*-alkoxylated phenyl groups and/or an electron-donating *N*,*N*′-dialkyl-amino substituent. This work shows that the long alkoxyl chains improve DSSC efficiency by creating dye insulation, reducing molecular aggregation, elevating porphyrin LUMOs, increasing open-circuit voltage of the devices, and possibly forming a blocking layer on the surface of TiO_2. Our studies also suggest that dodecoxyl chains provide a more complete insulation of the porphyrins than octoxyl and butoxyl chains. By applying these alkoxyl and alkyl chains, the LD16-sensitized solar cells outperform other dyes in this work with an overall efficiency of 10.24%.

Acknowledgements

We are grateful for the support from the National Science Council of Taiwan and for the computational resources from the National Center for High-Performance Computing, Taiwan.

Notes and references

1 M. K. Nazeeruddin, P. Péchy and M. Grätzel, *Chem. Commun.*, 1997, 1705–1706.
2 M. K. Nazeeruddin, S. M. Zakeeruddin, R. Humphry-Baker, M. Jirousek, P. Liska, N. Vlachopoulos, V. Shklover, C.-H. Fischer and M. Grätzel, *Inorg. Chem.*, 1999, **38**, 6298–6305.
3 M. K. Nazeeruddin, P. Péchy, T. Renouard, S. M. Zakeeruddin, R. Humphry-Baker, P. Comte, P. Liska, L. Cevey, E. Costa, V. Shklover, L. Spiccia, G. B. Deacon, C. A. Bignozzi and M. Grätzel, *J. Am. Chem. Soc.*, 2001, **123**, 1613–1624.
4 T. W. Hamann, R. A. Jensen, A. B. F. Martinson, H. V. Ryswykac and J. T. Hupp, *Energy Environ. Sci.*, 2008, **1**, 66–78.
5 L. M. Goncalves, V. de Zea Bermudez, H. A. Ribeiro and A. M. Mendes, *Energy Environ. Sci.*, 2008, **1**, 655–667.
6 M. K. Nazeeruddin, F. De Angelis, S. Fantacci, A. Selloni, G. Viscardi, P. Liska, S. Ito, B. Takeru and M. Grätzel, *J. Am. Chem. Soc.*, 2005, **127**, 16835–16847.
7 M. Grätzel, *Inorg. Chem.*, 2005, **44**, 6841–6851.
8 (*a*) F. Gao, Y. Wang, D. Shi, J. Zhang, M. Wang, X. Jing, R. Humphry-Baker, P. Wang, S. M. Zakeeruddin and M. Grätzel, *J. Am. Chem. Soc.*, 2008, **130**, 10720–10728; (*b*) C.-Y. Chen, M. Wang, J.-Y. Li, N. Pootrakulchote, L. Alibabaei, C.-H. Ngoc-le, J.-D. Decoppet, J.-H. Tsai, C. Grätzel, C.-G. Wu, S. M. Zakeeruddin and M. Grätzel, *ACS Nano*, 2009, **3**, 3103–3109; (*c*) Y. Cao, Y. Bai, Q. Yu, Y. Cheng, S. Liu, D. Shi, F. Gao and P. Wang, *J. Phys. Chem. C*, 2009, **113**, 6290; (*d*) Q. Yu, S. Liu, M. Zhang, N. Cai, Y. Wang, P. Wang, S. M. Zakeeruddin, P. Comte, R. Charvet, R. Humphry-Baker and M. Grätzel, *J. Phys. Chem. C*, 2009, **113**, 14559.
9 (*a*) W. M. Campbell, A. K. Burrell, D. L. Officer and K. W. Jolley, *Coord. Chem. Rev.*, 2004, **248**, 1363–1379; (*b*) H. Imahori, T. Umeyama and S. Ito, *Acc. Chem. Res.*, 2009, **42**, 1809–1818; (*c*) M. V. Martinez-Diaz, G. de la Torrea and T. Torres, *Chem. Commun.*, 2010, **46**, 7090–7108.
10 (*a*) S. Mathew, H. Iijima, Y. Toude, T. Umeyama, Y. Matano, S. Ito, N. V. Tkachenko, H. Lemmetyinen and H. Imahori, *J. Phys. Chem. C*, 2011, **115**, 14415–14424; (*b*) A. Kira, Y. Matsubara, H. Iijima, T. Umeyama, Y. Matano, S. Ito, M. Niemi, N. V. Tkachenko, H. Lemmetyinen and H. Imahori, *J. Phys. Chem. C*, 2010, **114**, 11293–11304; (*c*) H. Imahori, Y. Matsubara, H. Iijima, T. Umeyama, Y. Matano, S. Ito, M. Niemi, N. V. Tkachenko and H. Lemmetyinen, *J. Phys. Chem. C*, 2010, **114**, 10656–10665; (*d*) H. Imahori, S. Kang, H. Hayashi, M. Haruta, H. Kurata, S. Isoda, S. E. Canton, Y. Infahsaeng, A. Kathiravan, T. Pascher, P. Chabera, A. P. Yartsev and V. Sundstrom, *J. Phys. Chem. A*, 2011, **115**, 3679–3690; (*e*) H. Imahori, S. Hayashi, H. Hayashi, A. Oguro, S. Eu, T. Umeyama and Y. Matano, *J. Phys. Chem. C*, 2009, **113**, 18406–18413.
11 (*a*) C.-H. Lee, K. Chitre and E. Galoppini, *J. Chin. Chem. Soc.*, 2010, **57**, 1103–1110; (*b*) C.-H. Lee and E. Galoppini, *J. Org. Chem.*, 2010, **75**, 3692–3704; (*c*) N. R. de Tacconi, W. Chanmanee, K. Rajeshwar, J. Rochford and E. Galoppini, *J. Phys. Chem. C*, 2009, **113**, 2996–3006.

12 (*a*) W. M. Campbell, K. W. Jolley, P. Wagner, K. Wagner, P. J. Walsh, K. C. Gordon, L. Schmidt-Mende, M. K. Nazeeruddin, Q. Wang, M. Grätzel and D. L. Officer, *J. Phys. Chem. C*, 2007, **111**, 11760–11762; (*b*) A. J. Mozer, M. J. Griffith, G. Tsekouras, P. Wagner, G. G. Wallace, S. Mori, K. Sunahara, M. Miyashita, J. C. Earles, K. C. Gordon, L. Du, R. Katoh, A. Furube and D. L. Officer, *J. Am. Chem. Soc.*, 2009, **131**, 15621–15623.
13 T. Bessho, S. M. Zakeeruddin, C.-Y. Yeh, E. W.-G. Diau and M. Grätzel, *Angew. Chem., Int. Ed.*, 2010, **49**, 6646–6649.
14 G. Calogero, G. Di Marco, S. Caramori, S. Cazzanti, R. Argazzi and C. A. Bignozzi, *Energy Environ. Sci.*, 2009, **2**, 1162–1172.
15 (*a*) S. W. Park, D. S. Hwang, D. Y. Kim and D. Kim, *J. Chin. Chem. Soc.*, 2010, **57**, 1111–1118; (*b*) M. Ishida, S. W. Park, D. Hwang, Y. B. Koo, J. L. Sessler, D. Y. Kim and D. Kim, *J. Phys. Chem. C*, 2011, **115**, 19343–19354; (*c*) J. K. Park, J. Chen, H. R. Lee, S. W. Park, H. Shinokubo, A. Osuka and D. Kim, *J. Phys. Chem. C*, 2009, **113**, 21956–21963.
16 (*a*) C. Y. Lee, C. She, N. C. Jeong and J. T. Hupp, *Chem. Commun.*, 2010, **46**, 6090–6092; (*b*) R. A. Jensen, H. V. Ryswyk, C. She, J. M. Szarko, L. X. Chen and J. T. Hupp, *Langmuir*, 2010, **26**, 1401–1404; (*c*) C. Y. Lee and J. T. Hupp, *Langmuir*, 2010, **26**, 3760–3765.
17 I. Radivojevic, A. Varotto, C. Farleya and C. M. Drain, *Energy Environ. Sci.*, 2010, **3**, 1897–1909.
18 (*a*) C.-Y. Lin, C.-F. Lo, L. Luo, H.-P. Lu, C.-S. Hung and E. W.-G. Diau, *J. Phys. Chem. C*, 2009, **113**, 755–764; (*b*) C.-F. Lo, L. Luo, E. W.-G. Diau, I.-J. Chang and C.-Y. Lin, *Chem. Commun.*, 2006, 1430–1432; (*c*) L. Luo, C.-J. Lin, C.-Y. Tsai, H.-P. Wu, L.-L. Lin, C.-F. Lo, C.-Y. Lin and E. W.-G. Diau, *Phys. Chem. Chem. Phys.*, 2010, **12**, 1064–1071.
19 C.-Y. Lin, Y.-C. Wang, S.-J. Hsu, C.-F. Lo and E. W.-G. Diau, *J. Phys. Chem. C*, 2010, **114**, 687–693.
20 C.-F. Lo, S.-J. Hsu, C.-L. Wang, Y.-H. Cheng, H.-P. Lu, E. W.-G. Diau and C.-Y. Lin, *J. Phys. Chem. C*, 2010, **114**, 12018–12023.
21 C.-L. Wang, Y.-C. Chang, C.-M. Lan, C.-F. Lo, E. W.-G. Diau and C.-Y. Lin, *Energy Environ. Sci.*, 2011, **4**, 1788–1795.
22 Y.-C. Chang, C.-L. Wang, T.-Y. Pan, S.-H. Hong, C.-M. Lan, H.-H. Kuo, C.-F. Lo, H.-Y. Hsu, C.-Y. Lin and E. W.-G. Diau, *Chem. Commun.*, 2011, **47**, 8910–8912.
23 (*a*) K. E. Splan and J. T. Hupp, *Langmuir*, 2004, **20**, 10560–10566; (*b*) S. J. Lee, R. A. Jensen, C. D. Malliakas, M. G. Kanatzidis, J. T. Hupp and S. B. T. Nguyen, *J. Mater. Chem.*, 2008, **18**, 3640–3642; (*c*) S. J. Lee, C. D. Malliakas, M. G. Kanatzidis, J. T. Hupp and S. B. T. Nguyen, *Adv. Mater.*, 2008, **20**, 3543–3549.
24 (*a*) T. Ishizuka, L. E. Sinks, K. Song, S.-T. Hung, A. Nayak, K. Clays and M. J. Therien, *J. Am. Chem. Soc.*, 2011, **133**, 2884–2896; (*b*) T. N. Singh-Rachford, A. Nayak, M. L. Muro-Small, S. Goeb, M. J. Therien and F. N. Castellano, *J. Am. Chem. Soc.*, 2010, **132**, 14203–14211; (*c*) M. P. Nikiforov, U. Zerweck, P. Milde, C. Loppacher, T.-H. Park, H. T. Uyeda, M. J. Therien, L. Eng and D. Bonnell, *Nano Lett.*, 2008, **8**, 110–113.
25 M. Ikai, F. Ishikawa, N. Aratani, A. Osuka, S. Kawabata, T. Kajioka, H. Takeuchi, H. Fujikawa and Y. Taga, *Adv. Funct. Mater.*, 2006, **16**, 515–519.
26 (*a*) M. Freitag and E. Galoppini, *Energy Environ. Sci.*, 2011, **4**, 2482–2494; (*b*) M. Freitag and E. Galoppini, *Langmuir*, 2010, **26**, 8262–8269.
27 (*a*) N. Cai, S.-J. Moon, L. Cevey-Ha, T. Moehl, R. Humphry-Baker, P. Wang, S. M. Zakeeruddin and M. Grätzel, *Nano Lett.*, 2011, **11**, 1452–1456; (*b*) W. Zeng, Y. Cao, Y. Bai, Y. Wang, Y. Shi, M. Zhang, F. Wang, C. Pan and P. Wang, *Chem. Mater.*, 2010, **22**, 1915–1925.
28 J. Song, F. Zhang, C. Li, W. Liu, B. Li, Y. Huang and Z. Bo, *J. Phys. Chem. C*, 2009, **113**, 13391–13397.
29 N. Koumura, Z.-S. Wang, S. Mori, M. Miyashita, E. Suzuki and K. Hara, *J. Am. Chem. Soc.*, 2006, **128**, 14256–14257.
30 Q.-Y. Yu, J.-Y. Liao, S.-M. Zhou, Y. Shen, J.-M. Liu, D.-B. Kuang and C.-Y. Su, *J. Phys. Chem. C*, 2011, **115**, 22002–22008.
31 A. Yella, H.-W. Lee, H. N. Tsao, C. Yi, A. K. Chandiran, Md. K. Nazeeruddin, E. W.-G. Diau, C.-Y. Yeh, S. M. Zakeeruddin and M. Grätzel, *Science*, 2011, **334**, 629–634.
32 (*a*) K. Sonogashira, Y. Tohda and N. Hagihara, *Tetrahedron Lett.*, 1975, 4467–4470; (*b*) S. Takahashi, Y. Kuroyama and K. Sonogashira, *Synthesis*, 1980, 627–630.
33 M. Gouterman, *J. Mol. Spectrosc.*, 1961, **6**, 138.
34 M. Kasha, *Radiat. Res.*, 1963, **20**, 55–71.
35 C. Arunkumar, P. Bhyrappa and B. Varghese, *Tetrahedron Lett.*, 2006, **47**, 8033–8037.
36 (*a*) S. M. LeCours, S. G. DiMagno and M. J. Therien, *J. Am. Chem. Soc.*, 1996, **118**, 11854–11864; (*b*) S. M. LeCours, H. W. Guan, S. G. DiMagno, C. H. Wang and M. J. Therien, *J. Am. Chem. Soc.*, 1996, **118**, 1497–1503; (*c*) S. M. LeCours, C. M. Philips, J. C. D. Paula and M. J. Therien, *J. Am. Chem. Soc.*, 1997, **119**, 12578–12589.
37 (*a*) K. M. Kadish, E. V. Caemelbecke and G. Royal, in *The Porphyrin Handbook*, ed. K. M. Kadish, K. M. Smith and G. Guilard, Academic Press, New York, 2000, vol. 8, pp. 1–97; (*b*) K. M. Kadish, G. Royal, E. V. Caemelbecke and L. Gueletti, in *The Porphyrin Handbook*, ed. K. M. Kadish, K. M. Smith and G. Guilard, Academic Press, New York, 2000, vol. 9
38 *Materials Studio. Accelrys Materials Studio, v. 4.2*, Accelrys Inc, San Diego, CA, 2006.
39 (*a*) K. Kano, K. Fukuda, H. Wakami, R. Nishiyabu and R. F. Pasternack, *J. Am. Chem. Soc.*, 2000, **122**, 7494–7502; (*b*) K. Kano, T. Kakajima, M. Takei and S. Hashimoto, *Bull. Chem. Soc. Jpn.*, 1987, **60**, 1281–1287; (*c*) K. Kano, H. Minamizono, T. Kitae and S. Negi, *J. Phys. Chem. A*, 1997, **101**, 6118–6124.
40 (*a*) A. Burke, S. Ito, H. Snaith, U. Bach, J. Kwiatkowski and M. Grätzel, *Nano Lett.*, 2008, **8**, 977–981; (*b*) M.-H. Kim and Y.-U. Kwon, *J. Phys. Chem. C*, 2009, **113**, 17176–17182; (*c*) C. Sandquist and J. L. McHale, *J. Photochem. Photobiol., A*, 2011, **221**, 90–97; (*d*) P. Sudhagar, K. Asokan, J. H. Jung, Y.-G. Lee, S. Park and Y. S. Kang, *Nanoscale Res. Lett.*, 2010, **6**, 1–7; (*e*) N. Koumura, Z.-S. Wang, M. Miyashita, Y. Uemura, H. Sekiguchi, Y. Cui, A. Mori, S. Mori and K. Hara, *J. Mater. Chem.*, 2009, **19**, 4829–4836.

